

# Spin-flip effects on the Andreev bound states and supercurrents in a superconductor/quantum-dot/superconductor system

Hui Pan<sup>1</sup>, Tsung-Han Lin<sup>1</sup>, and Dapeng Yu<sup>1</sup>

<sup>1</sup>*State Key Laboratory for Mesoscopic Physics and Department of Physics,  
Peking University, Beijing 100871, China*

## Abstract

We investigate the spin-flip effects on the Andreev bound states and the supercurrent in a superconductor/quantum-dot/superconductor system theoretically. The spin-flip scattering in the quantum dot can reverse the supercurrent flowing through the system, and one  $\pi$ -junction transition occurs. By controlling the energy level of quantum dot, the supercurrent is reversed back and another  $\pi$ -junction transition appears. The different influences of the spin-flip scattering and the intradot energy level on the supercurrent are interpreted in the picture of Andreev bound states.

PACS number(s): 74.50.+r, 73.23.-b, 73.63.Kv

## I. INTRODUCTION

The superconductor coupled mesoscopic hybrid systems have attracted much attention in recent years, not only because of fundamental interest, but also of potential applications for future nanoelectronics.<sup>1,2,3,4</sup> In ballistic superconductor/normal-metal/superconductor (S/N/S) junction, Andreev bound states can be formed.<sup>5</sup> Each Andreev bound state carries a supercurrent in positive or negative direction at a given phase difference  $\phi$  between the two superconductors. Therefore, the net supercurrent between two superconductors depends not only on the phase difference  $\phi$ , but also on the occupation of the Andreev bound states. When two superconductors are weakly linked, the current-phase relation is  $I = I_c \sin(\phi)$ . On some occasions, the sign of  $I_c$  may be reversed,<sup>6</sup> which is referred to as the  $\pi$ -junction transition, because the minus sign can be absorbed in to the phase factor as  $\sin(\phi + \pi)$ .

The spin-orbit interaction plays an important role in the quantum dot (QD), because it can change the spin orientation of an electron. The spin-flip mechanisms in the GaAs-based QD have been studied.<sup>7</sup> The spin-flip effects on transport properties of a quantum dot in the normal-metal and superconductor hybrid system has been studied.<sup>8</sup> Various resonant peaks appear for the different spin-flip strengths in the QD.<sup>8</sup> The spin-dependent Andreev reflection tunneling through a QD with the spin-flip scattering has also been studied.<sup>9</sup> It is found that competition between the intradot spin-flip scattering and the tunneling coupling to the leads dominates the resonant behaviors of the Andreev reflection.<sup>9</sup>

It is natural to ask if the intradot spin-flip scattering could induce some novel phenomena in the supercurrent such as the  $\pi$ -junction transition. Motivated by this, we investigate the spin-flip scattering effects on the supercurrent and Andreev bound states in the superconductor/quantum-dot/superconductor (S/QD/S) system in this paper. By using the standard nonequilibrium Green's function (NGF) techniques,<sup>10,11,12,13</sup> we have analyzed quantum transport properties of the S/QD/S system. The configuration of the Andreev bound states depend heavily on the spin-flip strength. Since the supercurrent is carried by these states, the spin-flip scattering has a great influence on the amplitude and sign of the supercurrents. The dependence of the supercurrent and Andreev bound states on the gate voltage is also studied.

## II. PHYSICAL MODEL AND FORMULA

The S/QD/S system under consideration is described by the following Hamiltonian:

$$H = \sum_{\alpha=L,R} H_{\alpha} + H_{dot} + H_T, \quad (1)$$

with

$$H_{\alpha} = \sum_{k,\sigma} \epsilon_{\alpha,k} a_{\alpha,k\sigma}^{\dagger} a_{\alpha,k\sigma} + \sum_k [\Delta e^{-i\phi_{\alpha}} a_{\alpha,k\uparrow}^{\dagger} a_{\alpha,-k\downarrow}^{\dagger} + H.c.], \quad (2)$$

$$H_{dot} = \sum_{\sigma} \epsilon_0 d_{\sigma}^{\dagger} d_{\sigma} + r(d_{\uparrow}^{\dagger} d_{\downarrow} + d_{\downarrow}^{\dagger} d_{\uparrow}),$$

$$H_T = \sum_{\alpha,k\sigma} [t_{\alpha} a_{\alpha,k\sigma}^{\dagger} d_{\sigma} + H.c.],$$

where  $H_{\alpha}$  ( $\alpha = L/R$ ) is the standard BCS Hamiltonian for the left/right superconducting leads with phase  $\phi_L/\phi_R$  and the energy gap  $\Delta$ .  $H_{dot}$  models the quantum dot with a single spin-degenerate level  $\epsilon_0$ , which can be controlled by the gate voltage. The spin-flip term in the  $H_{dot}$  comes from the spin-orbit interaction in the quantum dot.  $H_T$  denotes the tunneling part of the Hamiltonian, and  $t_{L,R}$  are the hopping matrix. The supercurrent can be calculated from standard NGF techniques.

The  $4 \times 4$  Nambu representation is used to include the physics of AR and the spin-flip process in a unified formalism. The retarded Green's function is defined as  $G_{\alpha,\beta}^r(t, t') = \mp i\theta(\pm t \mp t') \langle \{\Psi_{\alpha}(t), \Psi_{\beta}^{\dagger}(t')\} \rangle$  with the operator  $\Psi_{\alpha} = (\psi_{\alpha\uparrow}^{\dagger}, \psi_{\alpha\downarrow}, \psi_{\alpha\downarrow}^{\dagger}, \psi_{\alpha\uparrow})^{\dagger}$ . Let  $g^r$  and  $G^r$  denote the Fourier-transformed retarded Green's function of the QD without and with the coupling to the leads. In the Nambu representation, they can be written as

$$(g^r(\epsilon))^{-1} = \begin{pmatrix} \epsilon - \epsilon_{0\uparrow} + i0^+ & 0 & -r & 0 \\ 0 & \epsilon + \epsilon_{0\downarrow} + i0^+ & 0 & r \\ -r & 0 & \epsilon - \epsilon_{0\downarrow} + i0^+ & 0 \\ 0 & r & 0 & \epsilon + \epsilon_{0\uparrow} + i0^+ \end{pmatrix}. \quad (3)$$

The retarded self-energy under the wide-bandwidth approximation can be derived as<sup>12,13</sup>

$$\Sigma_{L/R}^r(\epsilon) = -i\Gamma_{L/R}\rho(\epsilon) \begin{pmatrix} 1 & -\frac{\Delta}{\epsilon}e^{-i\phi_{L/R}} & 0 & 0 \\ -\frac{\Delta}{\epsilon}e^{i\phi_{L/R}} & 1 & 0 & 0 \\ 0 & 0 & 1 & \frac{\Delta}{\epsilon}e^{-i\phi_{L/R}} \\ 0 & 0 & \frac{\Delta}{\epsilon}e^{i\phi_{L/R}} & 1 \end{pmatrix}, \quad (4)$$

where  $\Gamma_{L/R}$  is the appropriate linewidth functions describing the coupling between the dot and the respective superconducting leads. Under the wide-bandwidth approximation, the linewidth functions are independent on the energy variable. Furthermore, we set  $\phi_L = \phi/2$  and  $\phi_R = -\phi/2$ ,  $\Gamma_L = \Gamma_R = \Gamma$  with small values for the symmetric and weak-coupling case. The factor  $\rho(\epsilon)$  is defined as

$$\rho(\epsilon) = \begin{cases} \frac{|\epsilon|}{(\epsilon^2 - \Delta^2)} & |\epsilon| > \Delta \\ \frac{|\epsilon|}{i(\Delta^2 - \epsilon^2)} & |\epsilon| < \Delta \end{cases}. \quad (5)$$

By using the Dyson equation, the retarded Green function of the system can be obtained as

$$G^r(\epsilon) = [g^{r^{-1}}(\epsilon) - \Sigma^r(\epsilon)]^{-1}, \quad (6)$$

where  $\Sigma^r = \Sigma_L^r + \Sigma_R^r$ . The Josephson current is expressed as

$$I_{L/R} = I_{L/R,\uparrow} + I_{L/R,\downarrow} = \frac{2e}{\hbar} \int \frac{d\epsilon}{2\pi} Tr\{\hat{\sigma}_z Re[G\Sigma_{L/R}]^<\}, \quad (7)$$

where  $[AB]^< \equiv A^<B^> + A^rB^<$  and  $\hat{\sigma}_z$  is a  $4 \times 4$  matrix with Pauli matrix  $\sigma_z$  as its diagonal components. In the steady transport, the current is

$$I = \frac{1}{2}(I_L - I_R) = \frac{e}{\hbar} \int \frac{d\epsilon}{2\pi} j(\epsilon) = \frac{e}{\hbar} \int \frac{d\epsilon}{2\pi} Tr\{\hat{\sigma}_z Re[G(\Sigma_L - \Sigma_R)]^<\}. \quad (8)$$

Applying the fluctuation-dissipation theorem, one has

$$G^<(\epsilon) = f(\epsilon)(G^a(\epsilon) - G^r(\epsilon)), \quad \Sigma_{L/R}^< = f(\epsilon)(\Sigma_{L/R}^a - \Sigma_{L/R}^r), \quad (9)$$

where  $f(\epsilon) = 1/(e^{\beta\epsilon} + 1)$  is the Fermi distribution function. Consequently, the Josephson current is expressed as

$$I = \frac{e}{\hbar} \int \frac{d\epsilon}{2\pi} f(\epsilon) j(\epsilon), \quad (10)$$

in which the current density  $j(\epsilon)$  is defined as

$$j(\epsilon) = Tr\{\hat{\sigma}_z Re[G^a(\Sigma_L^a - \Sigma_R^a) - G^r(\Sigma_L^r - \Sigma_R^r)]\}, \quad (11)$$

The analysis of the current carrying spectrum  $j(\epsilon)$  provides the information of the super-current carried by each of the Andreev bound state. The Josephson current can be divided into two parts, contributed by the continuous spectrum for  $|\omega| > \Delta$  and discrete spectrum for  $|\omega| < \Delta$ :

$$I = I_c + I_d, \quad (12)$$

$$I_c = \frac{e}{\hbar} \left( \int_{-\infty}^{-\Delta} + \int_{\Delta}^{\infty} \right) \frac{d\epsilon}{2\pi} f(\epsilon) j(\epsilon),$$

$$I_d = \frac{e}{\hbar} \int_{-\Delta}^{\Delta} \frac{d\epsilon}{2\pi} f(\epsilon) j(\epsilon).$$

The averaged LDOS is given by

$$D(\epsilon) = -\frac{1}{\pi} \text{Tr}\{ \text{Im}[G^r(\epsilon)] \}, \quad (13)$$

We perform the calculations at zero temperature in units of  $\hbar = e = 1$ . The energy gap of the superconductor is fixed as  $\Delta = 1$ . All the energy quantities in the calculations are scaled by  $\Delta$ . The linewidth is  $\Gamma = 0.1\Delta$  for the symmetric and weak-coupling case.

### III. RESULTS AND DISCUSSION

In the following, the numerical results of the supercurrents and the Andreev quasibound states are discussed in detail. The supercurrent originates from Andreev reflection at the interface between the superconducting leads and the central region. Fig. 1(a) and (b) present the supercurrent  $I$  (includes both  $I_c$  and  $I_d$ ) versus the phase difference  $\phi$  with different spin-flip scattering strength  $r$ . First, we investigate the case without the spin-flip scattering  $r = 0$ . The current  $I_d$  from the discrete spectrum vs  $\phi$  is similar to a  $\sin(\phi)$ -like curve. However, the current  $I_c$  from the continuous spectrum vs  $\phi$  is similar to a  $\sin(\phi + \pi)$ -like curve, because the current  $I_c$  is a  $\pi$ -junction Josephson relation<sup>14,15</sup>. Furthermore, the current  $I_d$  is much larger than the current  $I_c$ , which means that the total supercurrent  $I$  is mainly contributed by  $I_d$  and also shows a sine-like dependence on the phase  $\phi$ . Now, we investigate the case with the spin-flip scattering  $r = 0.2$ . It is interesting to point out that  $I$  vs  $\phi$  is not a  $\sin(\phi)$ -like but a  $\sin(\phi + \pi)$ -like curve. There is a  $\pi$ -junction transition for the supercurrent-phase relation. The reason is related to the spin-flip scattering which greatly suppresses the current  $I_d$ . Thus the total supercurrent is mainly contributed by  $I_c$  but not by  $I_d$  as that without the spin-flip scattering. Due to the quite different dependence of  $I_d$  and  $I_c$  on  $\phi$ , the supercurrent  $I$  shows a  $\pi$ -junction transition under the influence of the spin-flip scattering effects.

To fully understand the  $\pi$ -junction transition, we plot the  $j(\epsilon)$  for the cases with and without the spin-flip scattering in Fig. 1(c) and (d). For the case with  $r = 0$ , the original level  $\epsilon_0 = 0$  is split into two Andreev quasibound states. When the energy  $\epsilon$  of an incoming

electron lines up with the Andreev bound states, a resonance occurs, leading to a very large supercurrent. As seen from Fig. 1(c),  $j(\epsilon)$  has two  $\delta$ -function-type discrete spectra within the superconducting gap, corresponding to the two Andreev bound states. They carry supercurrents with opposite signs: positive for  $A_1$  and negative for  $A_{-1}$ .  $j(\epsilon)$  also has a continuous spectrum outside the superconducting gap: negative for  $C_{-1}$  and positive for  $C_1$ . At zero temperature, only the spectrum of  $\epsilon < 0$  relates to the current. Since the contribution from the discrete spectrum  $A_1$  is much larger than that from the continuous one  $C_{-1}$ , the current  $I$  is mostly contributed by  $I_d$ . For the case with  $r = 0.2$ , the original level  $\epsilon_0 = 0$  is split into two ones as  $\epsilon_{01}$  and  $\epsilon_{02}$  due to the spin-flip perturbation, which results in four Andreev bound states. The original Andreev bound state  $A_1$  is split into two ones as  $A_1$  and  $A_2$ , and similarly  $A_{-1}$  is split into  $A_{-1}$  and  $A_{-2}$ .  $j(\epsilon)$  has four  $\delta$ -function-type discrete spectra within the superconducting gap. The Andreev bound states depend strongly on the configuration of the QD levels ( $\epsilon_{01}, \epsilon_{02}$ ), but weakly on the phase difference  $\phi$ , and the electron levels  $\epsilon_{01}$  and  $\epsilon_{02}$  are coupled by Andreev reflection tunneling. Therefore, Andreev bound states can be viewed as hybrids of  $\epsilon_{01}$  and  $\epsilon_{02}$ . With increasing  $r$ ,  $A_1$  and  $A_{-2}$  move in the same direction, and both of them are below the Fermi level at strong enough  $r$ . As a consequence, they make little net contribution to the supercurrent, and the relatively small negative continuous spectrum of  $C_{-1}$  dominates. The contribution from the discrete spectrum is suppressed by the spin-flip scattering. This is the origin of the  $\pi$ -junction transition in the supercurrent under the influence of the spin-flip scattering in the QD. Another important quantity, the local density of states (LDOS)  $D(\epsilon)$ , is also shown in Fig. 1(e) and (f). A series of very narrow peaks emerge in  $D(\epsilon)$ , clearly indicating the formation of Andreev quasibound states inside the QD. The peaks of the current density  $j(\epsilon)$  are located precisely at the energies of Andreev bound states, which is a clear indication that the current is carried by these states.

The results above are obtained by fixing the intradot level  $\epsilon_0$  to zero, which is just at the center of the gap and at the Fermi level of both left and right leads. Next, we investigate how the supercurrent is affected when  $\epsilon_0$  is moved away from zero by the gate voltage. The supercurrent at different  $\epsilon_0$  are plotted in Fig. 2. As seen from Fig. 2(a), the supercurrent at  $\epsilon_0 = 0.1$  has similar  $\sin(\phi + \pi)$ -like phase dependence with that in Fig. 1(b). However, when  $\epsilon_0 = 0.3$ , there appears a  $\pi$ -junction transition, and then the supercurrent has similar  $\sin(\phi)$ -like phase dependence with that in Fig. 1(a). To explain this transition, the

corresponding current density  $j(\epsilon)$  are also shown in Fig. 2(c) and (d). With  $\epsilon_0 \neq 0$ , the Andreev quasibound states in  $j(\epsilon)$  are shifted in their positions. The two successive states are shifted in opposite directions. The two bound states  $A_1$  and  $A_2$  carrying the positive current move to  $-\Delta$ , while  $A_{-1}$  and  $A_{-2}$  carrying the negative current move to  $\Delta$ . At small  $\epsilon_0$ , the net current from discrete spectrum  $A_1$  and  $A_{-2}$  are very small and the continuous spectrum  $C_{-1}$  mainly contributes the current. At large enough  $\epsilon_0$ , the position of  $A_2$  and  $A_{-2}$  can even move past over the Fermi level, and both of their positions are below the Fermi level. Now, the current are mainly contributed by the discrete spectrum of  $A_1$  and  $A_2$ , but not by  $C_{-1}$  anymore. This is just the reason why the  $\pi$ -junction transition occurs. The corresponding  $D(\epsilon)$  shown in Fig. 2(e) and (f) are symmetric about the Fermi level. The narrow peaks with different height clearly indicate shift of the Andreev bound states.

To clearly show the  $\pi$ -junction transitions mentioned above, the dependence of  $I(\phi = \pi/2)$  on  $r$  and  $\epsilon_0$  are plotted in Fig. 3. As shown in Fig. 3(a),  $I(\pi/2)$  decreases slowly first with increasing  $r$ . When the spin-flip scattering strength  $r$  is comparable and close to  $\epsilon_0$ ,  $I(\pi/2)$  decreases rapidly and can even change the sign from positive to negative. Then the  $\pi$ -phase transition occurs as shown in Fig. 1. At larger  $\epsilon_0$ , the stronger  $r$  is needed to move the bound state  $A_{-2}$  to below the Fermi level as  $A_1$ . The negative current carried by  $A_{-2}$  counteracts with the positive current carried by  $A_1$ . Then the  $\pi$ -junction transition can occur. When there is no spin-flip scattering  $r = 0$ , increasing  $\epsilon_0$  can decrease  $I(\pi/2)$  as shown in Fig. 3(b). Because the intradot energy level  $\epsilon_{01}$  and  $\epsilon_{02}$  are not symmetric about the Fermi level at nonzero  $\epsilon_0$ , the Andreev reflection are suppressed and then the current decreases. For the nonzero  $r$ ,  $I(\pi/2)$  first increases and then decreases. At small spin-flip strength  $r$ , increasing  $\epsilon_0$  does not change of the sign of  $I(\pi/2)$ . At some strong enough  $r$ , which already induces the  $\pi$ -junction transition,  $I(\pi/2)$  can change the sign from negative to positive with increasing  $\epsilon_0$ . Then another  $\pi$ -phase transition occurs as shown in Fig. 2. When  $\epsilon_0$  is comparable and close to  $r$ , a maximum of  $I(\pi/2)$  appears. The reason is related to the position shift of the Andreev bound states with  $\epsilon_0$  as mentioned above. With increasing  $\epsilon_0$ ,  $A_1$  and  $A_2$  move to below the Fermi level while  $A_{-1}$  and  $A_{-2}$  move to above the Fermi level. The components contributed to the supercurrent change from  $(A_1, A_{-2}, C_{-1})$  to  $(A_1, A_2, C_{-1})$ , and then the current first increases. With further increasing  $\epsilon_0$ , the current density is suppressed greatly due to the asymmetry of the intradot levels, and then the current decrease again.

## IV. CONCLUSION

In summary, by using the nonequilibrium Green's function method, the spin-flip scattering effects on the supercurrent and Andreev bound states are studied in detail. The supercurrent is mostly contributed by the discrete Andreev bound states if there is no spin-flip scattering. The original Andreev bound state is split into two ones due to the spin-flip scattering, and the successive two bound states carrying currents with opposite signs move to the same direction with increasing spin-flip scattering strength. The main contributions to supercurrents can be changed from the discrete spectrum to the continuous spectrum at proper spin-flip scattering strength, which results in the  $\pi$ -junction transition. Furthermore, another  $\pi$ -junction transition can appear if the intradot energy level is controlled to some proper value by the gate voltage, because the successive two bound states carrying currents with the same signs move to the same direction. The main contributions to supercurrents are from the discrete spectrum again, which results in this transition. Although the strength of the spin-flip scattering and the position of the intradot energy level have quite different influence on the supercurrents, the two  $\pi$ -junction transition mechanisms are involved in the change of the current density.

### Acknowledgments

This project is supported by NSFC under Grants No. 90103027 and No. 50025206, and the National "973" Projects Foundation of China (No. 2002CB613505).

- 
- <sup>1</sup> D.C. Ralph, C.T. Black, and M. Tinkham, Phys. Rev. Lett. **74**, 3241 (1995).
  - <sup>2</sup> N. Knorr, M.A. Schneider, Lars Diekhoner, P. Wahl, and K. Kern, Phys. Rev. Lett. **88**, 096804 (2002).
  - <sup>3</sup> M.R. Buitelaar, T. Nussbaumer, and C. Schönenberger, Phys. Rev. Lett. **89**, 256801 (2002).
  - <sup>4</sup> H. Takayanagi, T. Akazaki, and J. Nitta, Phys. Rev. Lett. **75**, 3533 (1995).
  - <sup>5</sup> P.F. Bagwell, Phys. Rev. B **46**, 12573 (1992).
  - <sup>6</sup> J.J.A. Baselmans, A.F. Morpurgo, B.J. van Wees, and T.M. Klapwijk, Nature (London) **397**, 43 (1999).



- <sup>7</sup> A.V. Khaetskii and Y.V. Nazarov, Phys. Rev. B **61**, 12639 (2000); A.V. Khaetskii, Physica E (Amsterdam) **10**, 27 (2001).
- <sup>8</sup> Z. Chen, J. Wang, B. Wang, and D.Y. Xing, Phys. Lett. A **334**, 436 (2005).
- <sup>9</sup> X. Cao, Y. Shi, X. Song, S. Zhou, and H. Chen, Phys. Rev. B **70**, 235341 (2004)
- <sup>10</sup> A. L. Yeyati, A. Martin-Rodero, and J. C. Cruvas, Phys. Rev. B **54**, 7366 (1996).
- <sup>11</sup> A. L. Yeyati, J. C. Cuevas, A. Lopee-Davalos, and Martin-Rodero, Phys. Rev. B **55**, R6137 (1999).
- <sup>12</sup> Q.F. Sun, B.G. Wang, J. Wang, and T.H. Lin, Phys. Rev. B **61**, 4754 (1999).
- <sup>13</sup> Q.F. Sun, J. Wang, and T.H. Lin, Phys. Rev. B **62**, 3831 (648).
- <sup>14</sup> Th. Mühge, *et. al.* Phys. Rev. Lett. **77**, 1857 (1996)
- <sup>15</sup> D.J. van Harlingen, Rev. Mod. Phys. **67**, 515 (1995)

### Figure Captions

Fig. 1. The current  $I$  (solid line),  $I_d$  (dashed line), and  $I_c$  (dotted line) vs  $\phi$  for  $r = 0$  (a) and  $r = 0.2$  (b) with the dot level  $\epsilon_0 = 0$ . (c) and (d) are the corresponding  $j(\epsilon)$ , and (e) and (f) are the corresponding  $D(\epsilon)$ , respectively.

Fig. 2. The current  $I$  (solid line),  $I_d$  (dashed line), and  $I_c$  (dotted line) vs  $\phi$  for  $\epsilon_0 = 0.1$  (a) and  $\epsilon_0 = 0.2$  (b) with the spin-flip scattering strength  $r = 0.2$ . (c) and (d) are the corresponding  $j(\epsilon)$ , and (e) and (f) are the corresponding  $D(\epsilon)$ , respectively.

Fig. 3. (a) The current  $I(\pi/2)$  vs  $r$  at different  $\epsilon_0 = 0, 0.1, 0.2$  and  $0.3$ , respectively. (b) The current  $I(\pi/2)$  vs  $\epsilon_0$  at different  $r = 0, 0.1, 0.2$  and  $0.3$ , respectively.

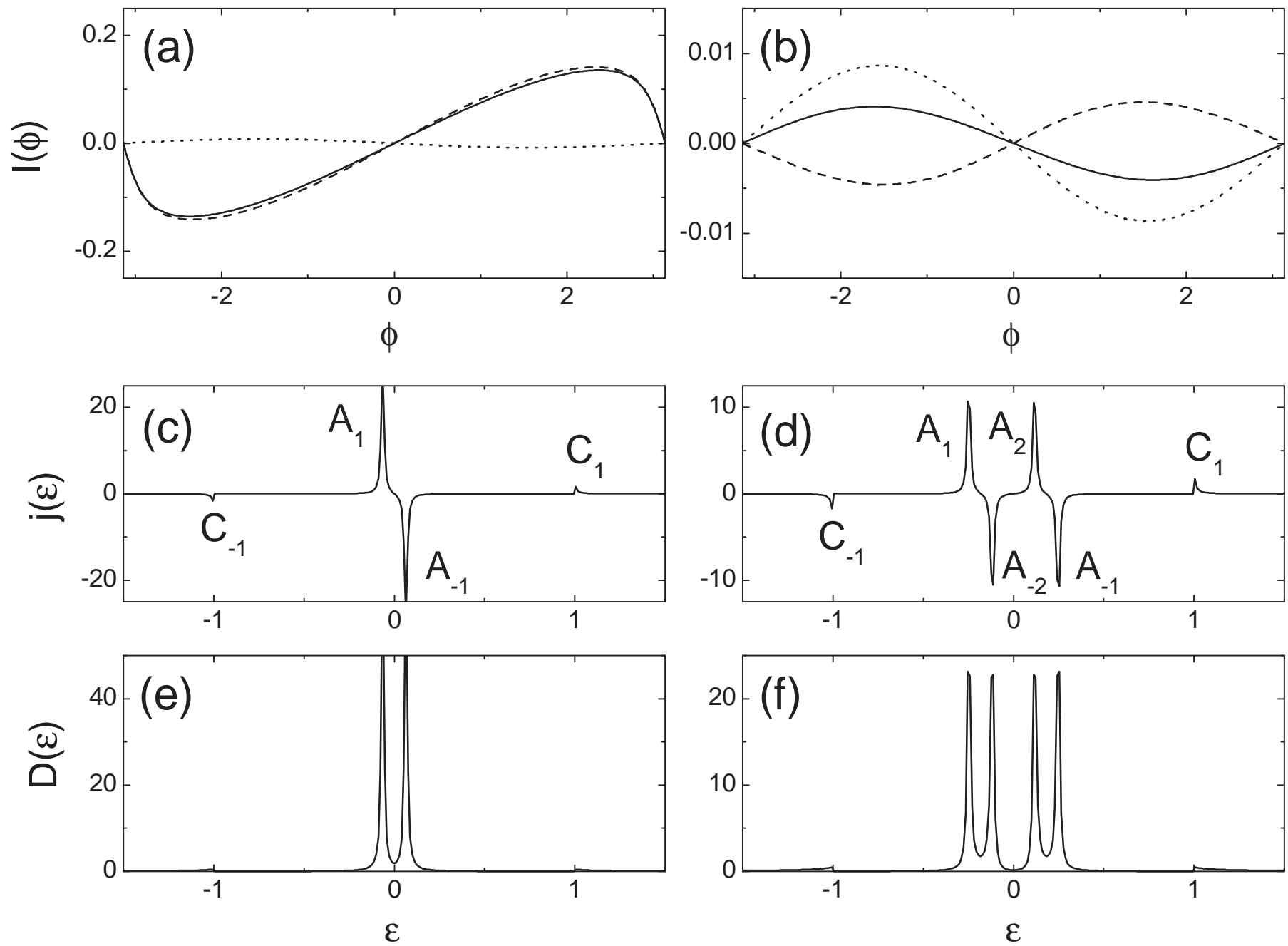


Fig. 1

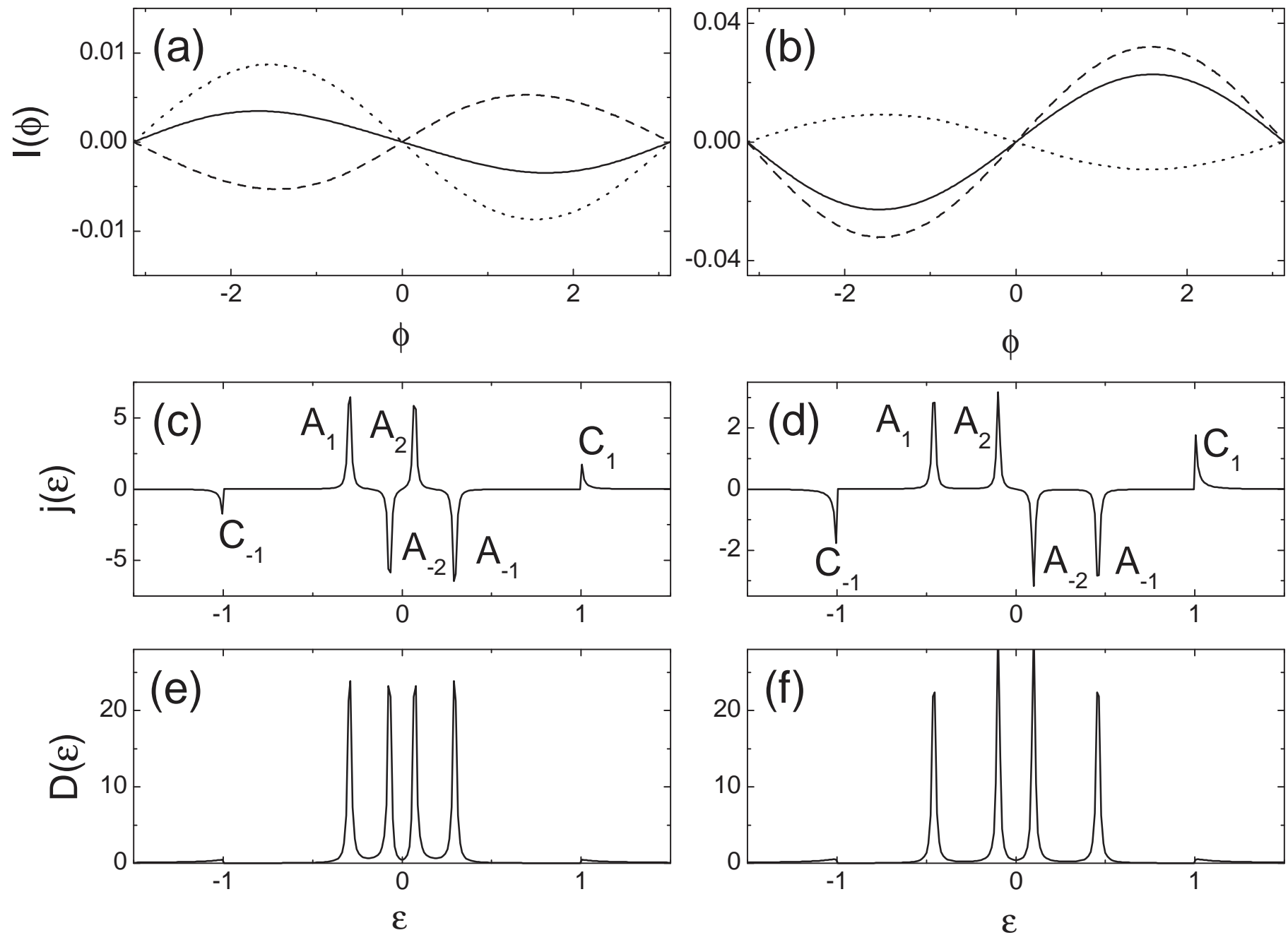


Fig. 2

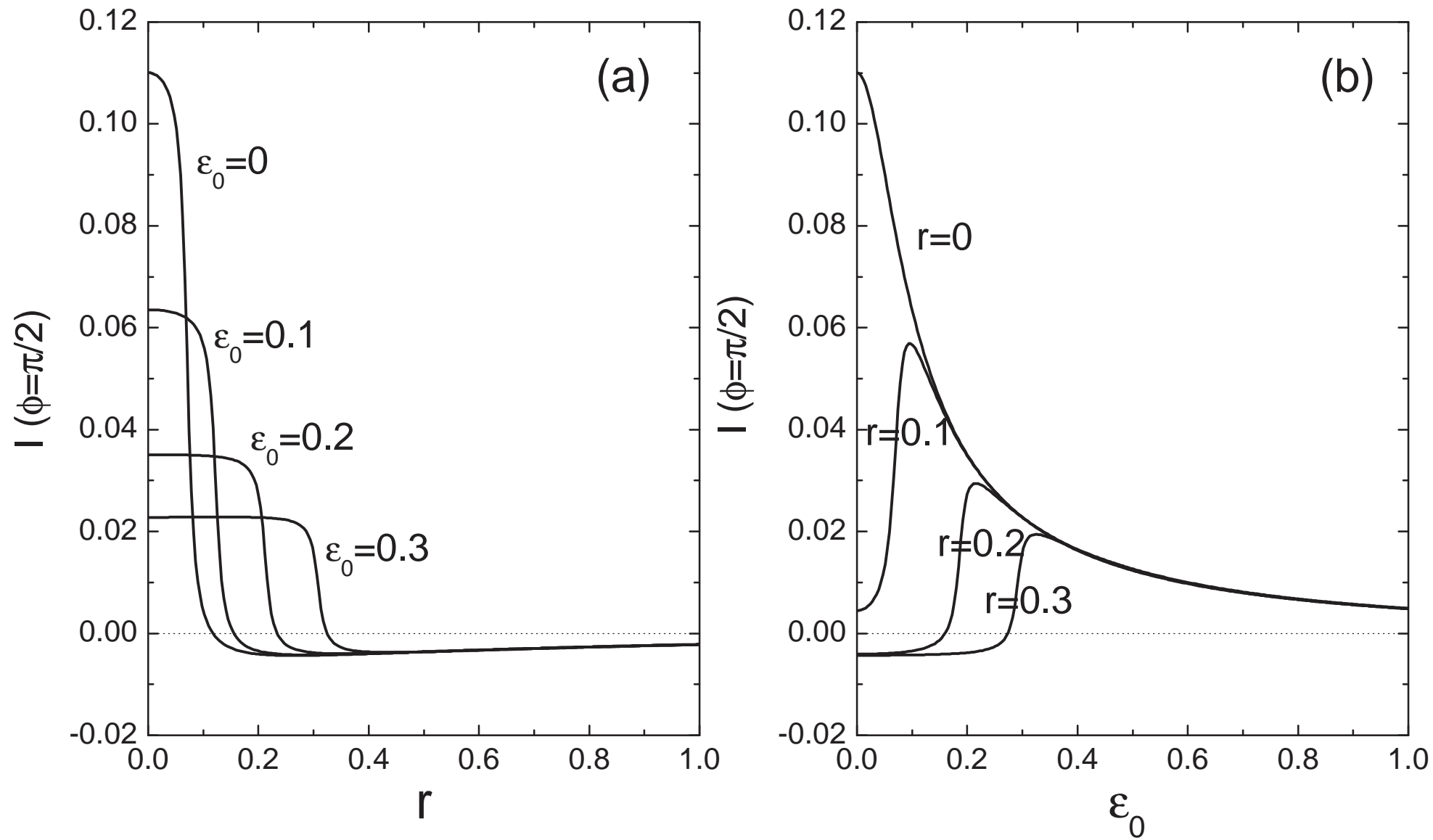


Fig. 3